Supporting Information

Finger et al. 10.1073/pnas.1418164112

SI Materials and Methods

Cell Lines. K457 and K3291 are derived from metastatic melanomas. K457 was provided by K. Brown (University of Arizona Cancer Center repository) and K3291 was generated by M. B. Powell. Tumor samples used to generate the lines were completely de-identified, and procurement was in compliance with institutional review board regulations. Cells were maintained in DMEM supplemented with 10% (vol/vol) FCS, 1% glutamine, and 1% penicillin-streptomycin. Stables were generated by treating cells with retrovirus containing scrambled shRNA or AKAP12 shRNA in pSiren-RetroQ (Clontech) and selected using 1.5 μg/mL puromycin.

shRNA Oligos. The shRNA oligos were as follows: AKAP12 shRNA2 (GATCCGGAGACTCCGATAAAGAGATTTCA AGAGAATC-TCTTTATCGGAGTCTCTTTTTTGCTAGCG, AATTCGCTAG-CAAAAAAGAGACTCC GATAAAGAGATTCTCTTGAAATC-TCTTTATCGGAGTCTCCG) and AKAP12 shRNA5 (GATCC-GAGACGGATGTAGTGTTGAATTCAAGAGA TTCAACACT-ACATCCGTCTTTTTTTGCTAGCG, AATTCGCTAGCAAAA-AAA GACGGATGTAGTGTTGAATCTCTTGAATTCAACACT-ACATCCGTCTCG).

Western Blots. Standard SDS-PAGE gels (5–15%) were run and blot probed using the following antibodies: AKAP12 (catalog no. sc-33577; Santa Cruz Biotechnology), pNDRG1 (catalog no. 5482; Cell Signaling), HSP-70 (catalog no. MA3-628; Thermo Scientific), tubulin (catalog no. 10R-T130A; Fitzgerald), and β-actin (catalog no. A5441; Sigma).

Low Attachment. A total of 100,000 K457 and K3291 cells were plated (in duplicate or triplicate) per well on 24-well ultra-low attachment plates and put at 21% O_2 or 0.5% O_2 over a time course. Total cell count was determined on the indicated days.

Colony Formation.

Clonogenic assay. K-457 (500 cells) and K-3291 (715 cells) cells were plated in DMEM + 10% (vol/vol) FBS into 60-mm dishes in triplicate. Plates were incubated at 37 °C in 5% CO_2 for ∼2 wk. Colonies were stained with crystal violet for 10 min and enumerated using a colony counter (Stuart Scientific).

Colony formation in soft agar. A total of 50,000 K-457 and K-3291 stable cells were plated in duplicate in six-well dishes in 0.7% noble agar on top of solidified 1.4% (wt/vol) agar, mixed with an equal volume of DMEM + 20% FBS. Normal DMEM + 10% (vol/vol) FBS was then put on top of the solidified agar. Cells were maintained at 37 °C in 5% CO_2 for 22 and 13 d, respectively. Multiple images of different fields were taken, and colony number was counted, averaged, and graphed with SEM.

3D growth in type I collagen. A total of 10,000 K457 stable cells were plated in 200 μL of DMEM + 10% (vol/vol) FBS and type I collagen at a 1:1 ratio. Cells are plated at 100 μL/well in a 48-well dish in duplicate and treated with DMSO, H-89 (15 μM), or Dasatinib (50 nM). Cells were grown at 37 °C in 5% CO_2 for ≥10 d. Pictures were taken under 10× magnification.

Migration. A total of 50,000 cells in SFM (serum-free media) were added to the upper chamber of fibronectin-coated transwells. The lower chamber was loaded with DMEM + 10% (vol/vol) FCS. After a 17- to 24-h incubation in 21%, 2%, or 0.5% O_2, the filters were scraped, and cells that migrated through were fixed, stained, and counted in three fields per filter under 10× magnification. DMSO, H-89 (15 μM), or Dasatinib (50 nM) was added to media/cells over the time course.

Wound Healing. Cells were grown to confluence, and a scratch wound was made using a p10 pipette tip. Fresh media were added with DMSO, H-89 (15 μM), or Dasatinib (50 nM), and wound closure was followed over time at 21% or 2% O_2. Photographs were taken at 4×, and relative wound closure was determined using Adobe Photoshop.

Invasion. A total of 50,000 K457 or 150,000–200,000 K3291 cells in SFM were added to the upper chamber of matrigel-coated invasion chambers. The lower chamber was loaded with regular media + 10% (vol/vol) FCS. After a 24-h incubation in 21% or 2% O_2, the filters were gently scraped, and cells that migrated through were fixed and stained. Cells were counted in three fields per filter under 10× magnification.

ChIP. Assays were performed as previously described (1), with the following modifications. Hypoxia-treated cells (0.5% O_2) were fixed in the chamber to avoid reoxygenation. HIF-1α IP was performed with 45 μg of sonicated chromatin and 10 μg of anti-HIF-1α antibody. Complexes were precipitated with 25 μL Dynabeads (1:1 protein A:G) for 2 h, followed by washes and elution from beads. Samples were run through the QIAquick PCR purification kit, and quantitative real-time PCR (qRT-PCR) was performed using a titration of pooled input samples as a standard curve. Signals were normalized to IgG, with Jumonji domain-containing protein 1A-HRE as a positive control, and an upstream region serving as a negative control. Sequences are available on request.

Immunohistochemistry. Slides were incubated at 60 °C for 30 min, followed by a wash with Xylene, 100% EtOH (×2), 90% EtOH, 80% EtOH, and 70% (vol/vol) EtOH, followed by a 5-min wash in H_2O. Slides were blocked for 10 min in 3% (vol/vol) H_2O_2, followed by a H_2O wash. Tissues were outlined with a PAP pen and blocked with 10% (vol/vol) NGS (normal goat serum) for 1 h in a humidified chamber. AKAP12 (Santa Cruz Biotechnology) was diluted in 10% NGS at 1:100 and added to tissues overnight in a humidified chamber at 4 °C. Slides were washed three times each for 5 min in PBS and incubated with biotinylated anti-rabbit diluted 1:200 in 10% NGS, for 30 min at in a humidified chamber. Tissue arrays were rinsed three times each for 5 min in PBS followed by a 30-min incubation with strep-HRP at 1:200. Another series of three times each for 5-min washes with PBS, incubation with AEC dye or DAB dye, and rinse in water was performed. Incubation with hematoxylin (Sigma-Aldrich) was performed last, followed by mounting. Tissue arrays (ME2082t and ME482t) were purchased from Biomax. Staining was scored by two independent observers and broken into no staining (0–0.5), low staining (0.6–1.5), and medium/high staining (1.6–3). Meca-32 staining was done in a similar manner as described above, but with the use of the Tyramide Signal Amplification (TSA) kit from Perkin-Elmer. Ki67 (NeoMarkers) staining was done as described above, but without a 60 °C incubation, and they were immersed in citric acid buffer, blocked with Avidin/Biotin, and diluted in PBT.

Immunofluorescence. K457 Scram cells were plated on coverslips in six-well dishes and exposed to 21% O_2 or 0.5% O_2 overnight. Slides were rinsed three times with PBS, fixed with 2% (vol/vol) paraformaldehyde for 20 min, and rinsed three times in PBS.

Cells were then permeabilized for 5 min with 0.1% Triton X-100 in PBS and three times with PBS rinses. A 1-h 1% BSA in PBS block was followed by primary antibody: AKAP12 at 1:75 (Santa Cruz Biotechnology) and PKA R2 at 1:50 (Abcam) for 1 h in 1% BSA in PBS. Cells were rinsed three times in PBS and incubated for 20 min with secondary antibody [Alexa Fluor 488 goat α-rabbit (Invitrogen) and Alexa Fluor 594 goat α-mouse (Molecular Probes)] in the dark, followed by 3xPBS rinses. DAPI was added at 1:10,000 for 1min, followed by rinsing three times with PBS. Coverslips were mounted using Fluoromount-G (Southern Biotech). Images were taken using a Leica DM6000B microscope at 100×. Exposure times for the red and green channels were kept consistent and were then put into Adobe Photoshop to make the final figures. Any changes in levels were kept consistent on the individual green and red channels across all images. DAPI was adjusted to obtain similar intensities between images. Pearson's correlation was used to determine overlap between AKAP12 and PKA-RII for individual cells in the original images using Image Pro Premier software, and then values were averaged and presented as average ± SEM.

qRT-PCR. A total of 1–1.5 μg of total RNA was reverse transcribed with Moloney murine leukemia virus reverse transcriptase (Invitrogen) or the iScript cDNA synthesis kit (Bio-Rad) according to the manufacturer's instructions. Approximately 0.5% of each RT reaction was added to qRT-PCR reactions containing the following: 5 μL 2× SYBR Green mastermix (ABI) and 0.2 μL each of 10 μM forward and reverse primers specific for the genes of interest in a total volume of 10 μL. The qRT-PCR reactions were done using the ABIPRISM 7900 sequence detection system, and expression levels were calculated using the relative standard curve method to determine RNA quantity, normalized to 18S. Sequences are available on request.

In Vivo.

Tail vein. A total of 7×10^5 K457 cells in 100 μL sterile PBS were injected into the tail vein of 4-wk-old female SCID mice (Charles River Laboratories). The lung was fixed in 10% (vol/vol) formalin followed by fixation in paraffin. Percent tumor burden was calculated as an average of tumor to normal area, which was obtained by examining three fields from three nonserial H&E sections from each mouse using ImageJ.

A total of 1×10^6 K3291 cells in 100 μL sterile PBS were injected into the tail vein of 4.5-wk-old male SCID mice. After approximately 6 wk, mice were killed, and the lungs were collected. Percent tumor burden was calculated as an average of tumor to normal area, which was obtained by examining five fields from H&E sections from each mouse using ImageJ. Mice were maintained and cared for under approval of the Institutional Animal Care and Use Committee at Stanford University.

Orthotopic. A total of 1×10^6 K457 cells per mouse were injected intradermally into female *nu/nu* mice (Charles River Laboratories). Calipers were used to measure primary tumor size in two dimensions, and tumor volume was calculated as $W^2 \times L \times 0.5$ (where W = shortest of two measurements). Sixty-three days after tumor cell injections, mice were anesthetized with a ketamine/xylazine mixture, the primary tumor was removed, and the wound was sutured closed. Mice were monitored and followed over a 34-wk time course, and any recurrent tumor was removed in the same manner. Immunohistochemistry was performed as described above. Staining for hypoxia in vivo was done using the Hypoxyprobe-1 Omni Kit (Hypoxyprobe).

CT scans. Mice were anesthetized with 2% isofluorane and 4 L/min oxygen and imaged on a CT scanner (Gamma Medica-Ideas). Images were acquired for 1 min with a 75-kV and 225-μA beam and then reconstructed using a voxel size of 0.17 mm and a field of view of 110 mm.

Apoptosis.

TUNEL. Staining on in vivo tissues was done following the DeadEnd Fluorometric TUNEL System protocol (catalog no. G3250; Promega).

APO-BRDU. Flow cytometry was done to determine apoptosis on in vitro cells stained using the APO-BRDU kit (catalog no. 556405; BD Biosciences), following the recommended protocol and analyzed using FlowJo software.

TCGA Analysis. To evaluate the mRNA expression level of AKAP12 isoforms in human melanoma samples, we extracted the RNAseq-based expression values of isoform 1 (exon 1, chr6:151561134–151561194:+; exon 2, chr6:151561509–151561859:+; exon 3, chr6:151626882–151627038:+) and isoform 2 (exon 4, chr6:151646666–151647020:+) from the TCGA Skin Cutaneous Melanoma dataset analyzed by IlluminaHiSeq for exon expression (386 samples) and then aligned them with the available patient clinical data (TCGA May 16, 2014 update). Examples of other cancer studies using the TCGA database are referenced here (2, 3).

Phosphoproteomic Screen. Sample collection, mass spectrometry, and data and bioinformatics analysis were done as described previously (4). Additional related references for targeted-phosphoproteomic approach are cited elsewhere (5–7).

Structural analysis. The N-terminal 200 amino acid residues of human AKAP12 isoform 1 (National Center for Biotechnology Information accession no. NP_005091) were submitted to QUARK (zhanglab.ccmb.med.umich.edu/QUARK/) for ab initio protein folding and protein structure prediction (8). Model 1 of the predicted structures, with a template modeling score of 0.2795 ± 0.0833 (zhanglab.ccmb.med.umich.edu/TM-score/), was visualized in University of California, San Francisco, Chimera (version 1.8rc) for structural illustration. The myristoylation motif (amino acid residues 1–15) is colored in red (9). The rest of the 106 amino acid residues unique to isoform 1 are colored in green. Sequence alignment was done using AlignX.

Protein–protein docking was performed using HADDOCK web server (haddock.science.uu.nl/services/HADDOCK/haddock.php) and "the Easy interface" parameters (10). The crystal structure of cAMP-dependent PKA regulatory subunit was retrieved from the Protein Data Bank (PDB, www.rcsb.org) with ID code 3IM4. The AKAP anchoring helix of human AKAP12 isoform 1 was derived according to the sequence ELETKSSKLVQNIIQTAVD (11, 12).

Statistics. Unless otherwise noted, significance was determined by a Student t test. $P \leq 0.05$ was considered significant.

1. Krieg AJ, et al. (2010) Regulation of the histone demethylase JMJD1A by hypoxia-inducible factor 1 alpha enhances hypoxic gene expression and tumor growth. *Mol Cell Biol* 30(1):344–353.
2. Cancer Genome Atlas N; Cancer Genome Atlas Network (2012) Comprehensive molecular characterization of human colon and rectal cancer. *Nature* 487(7407):330–337.
3. Cancer Genome Atlas Research Network (2008) Comprehensive genomic characterization defines human glioblastoma genes and core pathways. *Nature* 455(7216):1061–1068.
4. Gnad F, et al. (2013) Systems-wide analysis of K-Ras, Cdc42, and PAK4 signaling by quantitative phosphoproteomics. *Mol Cell Proteomics* 12(8):2070–2080.
5. Stokes MP, et al. (2012) PTMScan direct: Identification and quantification of peptides from critical signaling proteins by immunoaffinity enrichment coupled with LC-MS/MS. *Mol Cell Proteomics* 11(5):187–201.
6. Carretero J, et al. (2010) Integrative genomic and proteomic analyses identify targets for Lkb1-deficient metastatic lung tumors. *Cancer Cell* 17(6):547–559.
7. Zhang H, et al. (2002) Phosphoprotein analysis using antibodies broadly reactive against phosphorylated motifs. *J Biol Chem* 277(42):39379–39387.
8. Xu D, Zhang Y (2012) Ab initio protein structure assembly using continuous structure fragments and optimized knowledge-based force field. *Proteins* 80(7):1715–1735.

9. Streb JW, Kitchen CM, Gelman IH, Miano JM (2004) Multiple promoters direct expression of three AKAP12 isoforms with distinct subcellular and tissue distribution profiles. *J Biol Chem* 279(53):56014–56023.
10. de Vries SJ, van Dijk M, Bonvin AM (2010) The HADDOCK web server for data-driven biomolecular docking. *Nat Protoc* 5(5):883–897.
11. Gold MG, et al. (2013) Engineering A-kinase anchoring protein (AKAP)-selective regulatory subunits of protein kinase A (PKA) through structure-based phage selection. *J Biol Chem* 288(24):17111–17121.
12. Wen J, Scoles DR, Facelli JC (2014) Structure prediction of polyglutamine disease proteins: Comparison of methods. *BMC Bioinformatics* 15(Suppl 7):S11.

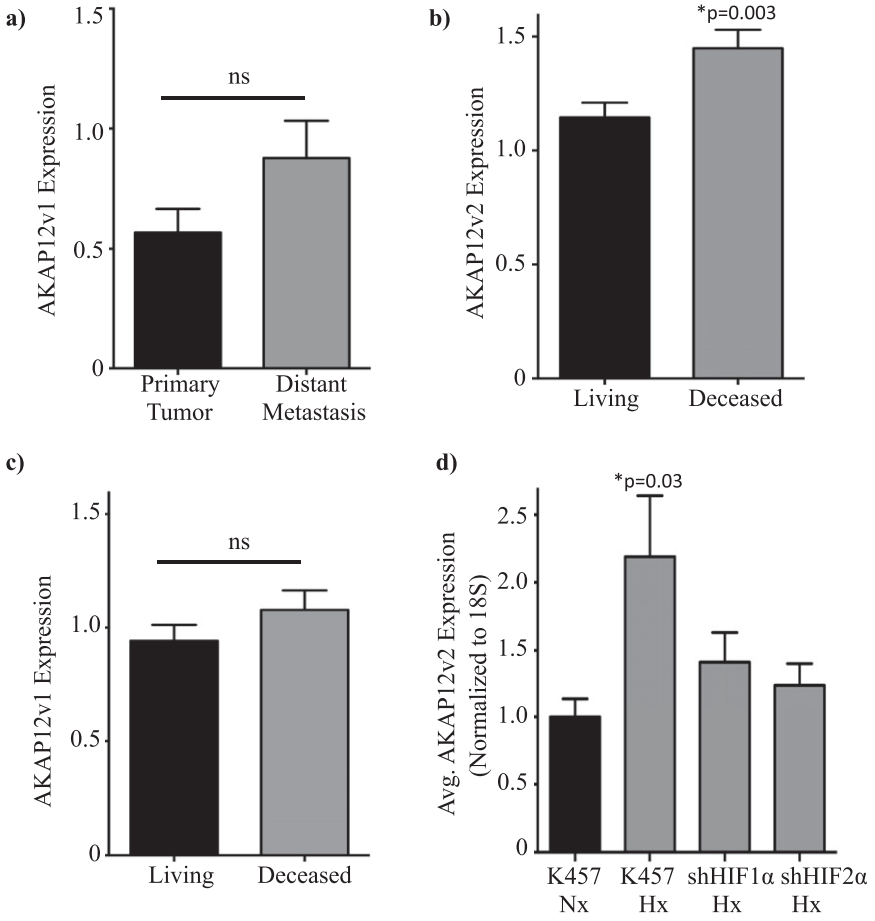

Fig. S1. AKAP12v2 is significantly linked to human metastatic disease. (*A*) AKAP12v1 expression is not significantly different in primary tumor patient ($n = 74$) samples vs. distant metastasis ($n = 39$). (*B* and *C*) AKAP12v2, but not AKAP12v1, expression is significantly elevated in patients who were deceased ($n = 148$) vs. living ($n = 214$) at the last follow-up time point. Graph is average expression ± SEM (*$P = 0.003$, two-tailed *t* test). (*D*) qRT-PCR examining hypoxic induction of AKAP12v2 with shHIF1α and shHIF2a in K457 cells. Graph is the average ± SEM of two experiments, each normalized to 18S and K457 cells under normoxic conditions (*$P = 0.03$, two-tailed *t* test).

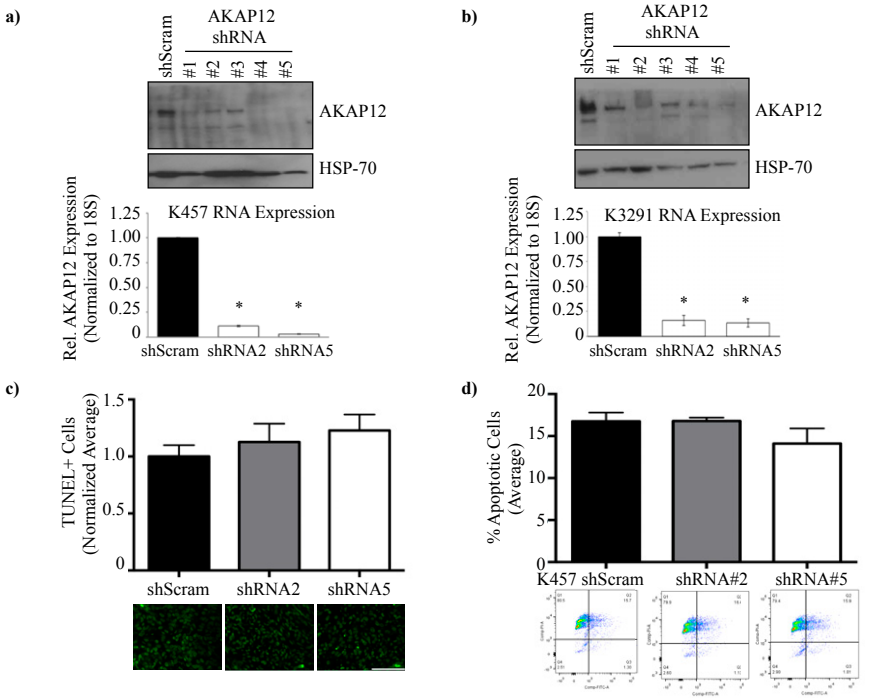

Fig. S2. AKAP12 knockdown does not affect apoptosis. (*A*) Western blot to demonstrate stable knockdown of AKAP12 at the protein level using five shRNAs in the K457 metastatic melanoma cell line. AKAP12 shRNA2 and shRNA5 were used for experiments in the paper. Confirmation of AKAP12 knockdown, using the two selected shRNAs, is demonstrated at the RNA level through qRT-PCR ($P < 0.01$, two-tailed *t* test). (*B*) Western blot and qRT-PCR demonstrate stable knockdown of AKAP12 in K3291 metastatic melanoma cells, as describe in *A*. (*C*) Tumor tissues were stained, and the percent TUNEL+ cells was calculated for three fields per mouse and normalized to the shScram group. Representative images taken at 63×. (Scale bar, 75 μm.) (*D*) Average percent apoptoic cells (in vitro) under hypoxia (0.5% O_2). Graph and plots are representative of three independent experiments.

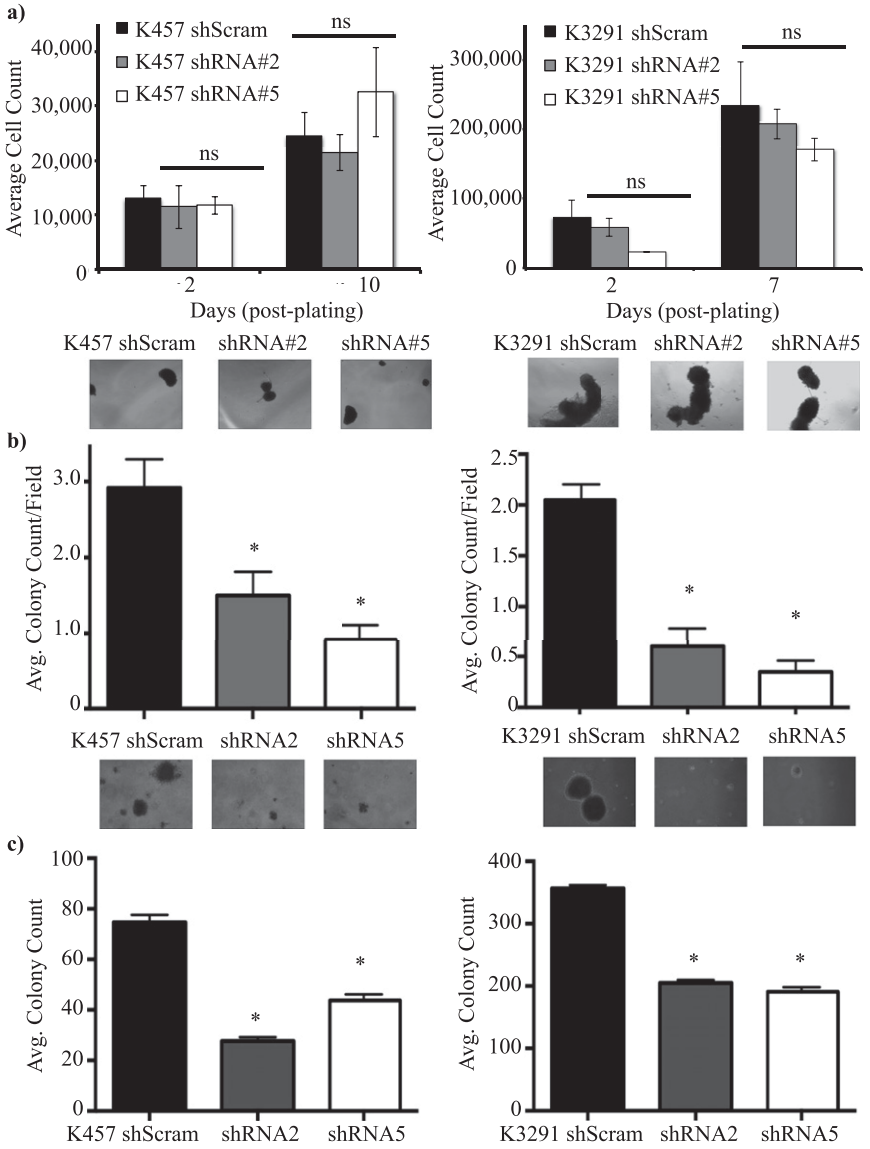

Fig. S3. AKAP12 affects growth under attachment conditions, but not under low-attachment conditions. (*A*) K457 and K3291 cells were grown on ultra-low attachment plates under hypoxic (0.5% O_2) conditions, and total cell number was counted over the indicated time course. Graph is a representative experiment from three or more independent experiments. Representative images at 4×. (*B*) K457 and K3291 cells were plated in agar, and the average colony count per field is graphed from representative experiments. Two-tailed *t* test, $*P < 0.01$. (*C*) Cells were plated in triplicate, and the average colony count from a representative experiment is graphed. Two-tailed *t* test ($*P < 0.01$).

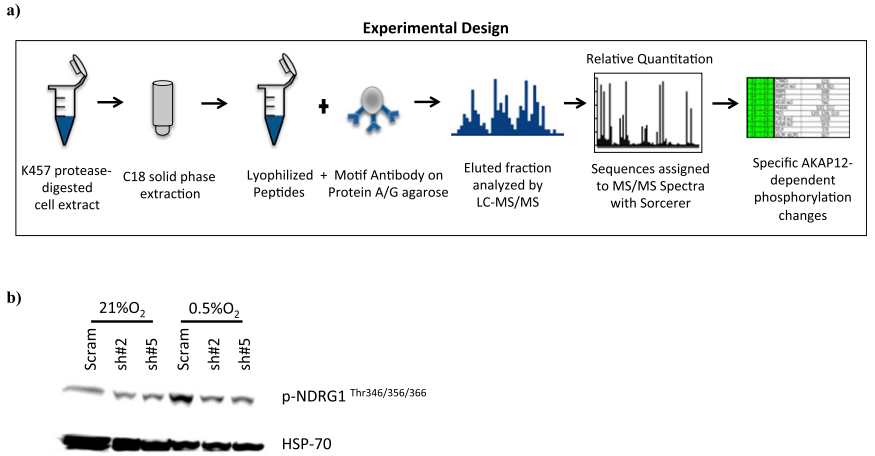

Fig. S4. Outline of kinome-wide phosphoscreen. (*A*) Outline of phospho-screen performed using K457 cells. Cells were protease digested, underwent solid phase extraction, followed by incubation with motif antibodies, run through MS, and analyzed for oxygen and AKAP12-dependent phosphorylation changes. Diagram based on previous description of the method (5). (*B*) We verified one of the specific phosphorylation events from our study with a Western blot showing pNDRG1 in AKAP12-expressing cells under hypoxia.

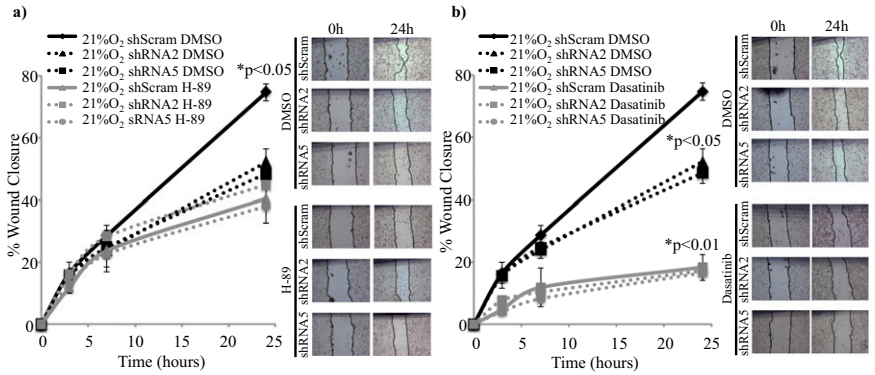

Fig. S5. AKAP12 regulates metastatic melanoma cell migration. (*A* and *B*) K457 stable cells were plated to confluence, a scratch wound was made, and wound closure was followed over time. Cells were treated with DMSO, H-89 (15 μM), or Dasatinib (50 nM). Representative images and graphs ± SEM are shown.

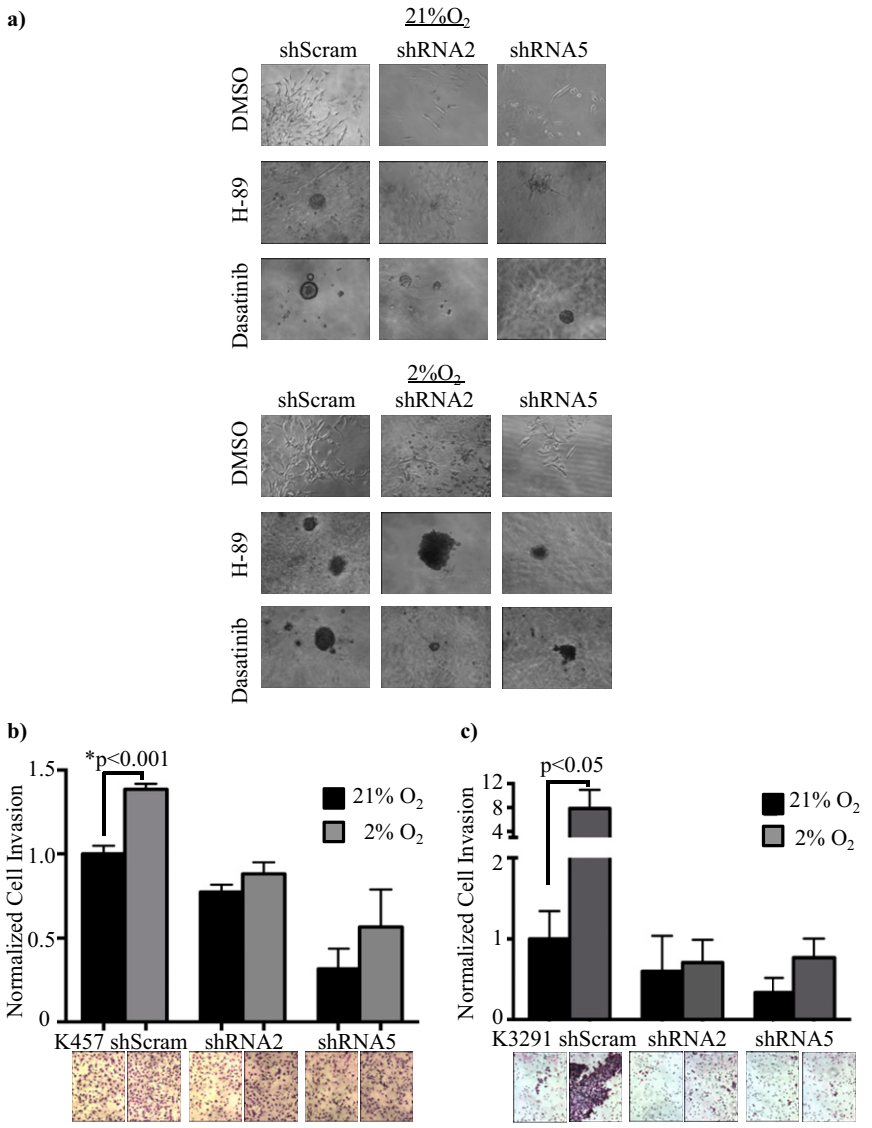

Fig. S6. AKAP12 regulates invasive potential of metastatic melanoma cells. (*A*) K457 cells were grown 3D in collagen under normoxia (21% O_2) or hypoxia (2% O_2). Invasive potential was determined by the ability to degrade collagen (track-like formations). Cells were treated with DMSO, H-89 (15 μM), or Dasatinib (50 nM). Images are representative of three independent experiments. (*B*) K457 shScram or shAKAP12 cells that invaded through matrigel-coated invasion chambers when exposed to 21% O_2 and 2% O_2 were fixed, stained, and counted. Graph is the average ± SEM of two independent trials (two-tailed *t* test). Representative images are shown. (*C*) K3291 shScram or shAKAP12 cells that invaded through matrigel-coated invasion chambers when exposed to 21% O_2 and 2% O_2 were fixed, stained, and counted. Graph is the average ± SEM of two independent trials (two-tailed *t* test). Representative images are shown.

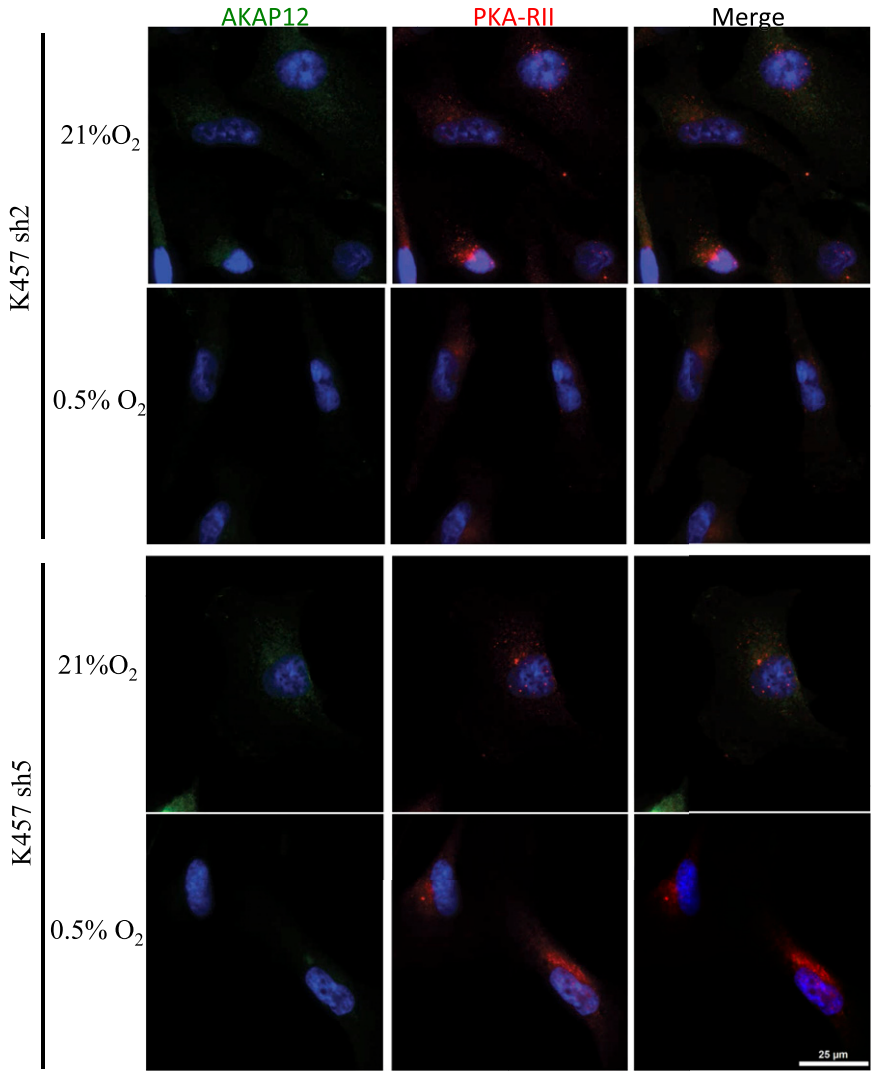

Fig. S7. AKAP12 staining is weak in K457 shAKAP12 cells. Control experiment in which K457 sh2 and sh5 cells were stained for AKAP12 (green) and PKA-RII (red). Weak staining was detected in cells with AKAP12 knocked down. Images taken at 100×. (Scale bar, 25 μm.)

Table S1. Kinome-wide AKAP12-dependent phosphorylation changes

K457 AKAP12 shRNA#5/K457 Scram shRNA	K457 AKAP12 shRNA#2/K457 Scram shRNA	K457 AKAP12 shRNA#5/K457 Scram shRNA	K457 AKAP12 shRNA#2/K457 Scram shRNA	Protein	Phosphorylation
Repressed at normoxia (21% O_2)		Repressed at hypoxia (0.5% O_2)			
Induced at normoxia (21% O_2)		Induced at hypoxia (0.5% O_2)			
3.3	2.5	2.0	1.9	CTNND1	S230
2.9	2.9	1.2	1.4	ADAM22 iso2	S819
2.9	2.9	1.2	1.4	ADAM22 iso2	S821
2.5	3.2	2.4	1.4	RBBP6	S688
4.4	6.1	1.2	1.2	RNPC2	S136
2.9	3.5	2.2	1.5	AS160 iso3	T642
3.0	3.2	−1.6	−3.2	PRAS40	S202
3.0	3.2	−1.6	−3.2	PRAS40	S212
2.8	4.2	1.9	3.4	PKD1	S205, S208
2.8	4.2	1.9	3.4	PKD1	S205, T210
4.7	2.6	4.5	5.2	CHD-8 iso2	S2008
2.5	9.5	3.2	3.1	RoXaN iso2	S476
4.1	3.3	2.5	3.3	SELH	S78
2.6	2.9	3.2	2.8	abLIM; abLIM2	S677
−1.0	2.6	8.4	5.7	abLIM3	S650
1.2	1.5	3.3	2.5	SIPA1L2 iso2	S1472
1.7	2.1	15.8	10.6	SIPA1L2 iso2	S1611
1.7	2.1	15.8	10.6	SIPA1L2 iso2	T1616
1.3	1.1	3.7	3.3	Abi-2 iso2	S285
1.3	1.1	3.7	3.3	Abi-2 iso2	S291
1.4	1.7	2.9	2.6	TANC1	S313
1.7	1.9	5.0	4.4	TANC1	S319
−1.0	−1.2	3.5	2.7	tensin 3	S660
−1.0	−1.2	3.5	2.7	tensin 3	S662
−2.3	2.4	3.6	2.7	PLXNC1	S978
−2.3	−1.2	5.3	5.7	FADD	S41
−1.3	1.4	3.7	4.2	CEP170 iso2	S832
−1.3	1.4	3.7	4.2	CEP170 iso2	S845
−1.4	−1.2	2.9	2.5	RXRG	S222
1.5	2.1	11.7	14.8	INF2 iso2	S1076
1.3	2.0	8.4	12.1	INF2 iso2	S1077
2.1	2.1	2.6	2.6	MYO18A iso4	S1068
1.4	1.9	5.5	4.1	SSFA2	S737
1.1	1.6	4.7	3.1	SSFA2	S752
1.2	1.3	2.6	2.5	TUBB	T312
1.3	−1.2	7.4	4.6	ATIC	S313
−1.2	1.0	25.3	21.4	MTHFD1	T417
1.1	1.1	4.2	4.4	MTHFD1	T77
−2.6	2.2	5.2	2.8	PCYT1A	S331
1.6	1.6	5.0	7.2	UGP2	S448
1.6	4.5	5.1	3.4	UMPS	S172
−1.1	−1.3	3.4	2.7	DAB2IP iso6	S1031
2.0	3.0	3.8	2.6	GPSM1	S469
1.6	2.5	4.4	2.5	RGL2	S187
1.5	1.5	3.0	3.3	TBC1D5	S584
1.2	1.4	2.8	3.1	PLEKHA5	S55
1.2	1.4	2.8	3.1	PLEKHA5	T56
−3.1	1.2	2.5	2.8	PAN3	S368
−1.7	1.2	15.0	11.8	CDK12	S276
2.0	1.4	2.7	3.8	GCN2	S254
1.4	1.6	4.6	2.5	GCK	T174
−1.3	1.5	15.6	12.9	HGK	T187
1.5	1.2	2.7	2.8	PKD2	S198
1.1	1.4	3.2	2.6	p90RSK iso3	S380
1.1	1.7	3.6	2.5	Abl; Bcr/Abl	T1000
1.1	1.7	3.6	2.5	Abl; Bcr/Abl	S1007
1.1	1.7	3.6	2.5	Abl; Bcr/Abl	T1008
1.1	1.7	3.6	2.5	Abl; Bcr/Abl	S1011
−1.0	−1.1	3.5	2.7	ZAP	S590

Table S1. Cont.

K457 AKAP12 shRNA#5/K457 Scram shRNA	K457 AKAP12 shRNA#2/K457 Scram shRNA	K457 AKAP12 shRNA#5/K457 Scram shRNA	K457 AKAP12 shRNA#2/K457 Scram shRNA	Protein	Phosphorylation
−1.0	−1.1	3.5	2.7	ZAP	S593
−1.0	−1.1	3.5	2.7	ZAP	S594
1.5	3.4	8.4	5.2	ABCA6	T755
−1.4	−1.2	3.6	4.1	DENND4C	S1402, S1426
−1.4	−1.2	3.6	4.1	DENND4C	S1404, S1426
−1.4	−1.2	3.6	4.1	DENND4C	S1404, S1430
−1.3	1.2	3.6	3.3	GPR64	T190
1.3	1.0	4.3	3.1	OSBPL6 iso4	T288
1.3	1.3	5.1	2.8	OSBPL6 iso4	S290
−1.6	−1.9	5.4	3.5	PIGX	S136
1.7	1.6	3.4	2.5	TMC8	Y238, S248, S249
−6.2	1.6	3.4	2.8	TMEM192	S230
1.1	−1.5	5.7	3.9	SGT1	S477
2.6	1.1	2.7	3.6	FLNA	S2163
−2.1	−3.8	10.7	7.6	NOLC1	S681
−2.1	−3.8	10.7	7.6	NOLC1	Y682
1.4	1.7	3.9	4.9	Per3	S940
2.0	1.7	2.7	5.0	TAZ	S117
2.4	2.2	6.9	12.8	TAZ	Y118
1.0	1.3	5.6	4.4	RBBP7	S258
1.0	1.3	5.6	4.4	RBBP7	T261
1.0	1.3	5.6	4.4	RBBP7	S265
−2.3	−1.2	3.7	4.1	UBE2L6	S26
−1.2	1.2	3.9	2.7	FAM117B	S219
−1.3	−1.2	3.4	3.4	FAM91A1	S754
−1.7	−1.3	3.8	2.6	OVCA2	S168
1.7	1.6	2.5	2.7	PRR14	T363
1.0	1.3	8.3	5.6	SNX18	T572
2.5	2.0	3.9	2.5	VIPAS39	T104
2.5	2.0	3.9	2.5	VIPAS39	S105
2.5	2.0	3.9	2.5	VIPAS39	T106
−3.0	−3.9	1.8	2.6	UBXN7	S464
−4.2	−2.9	−2.5	2.5	FAT10	S110
−4.2	−2.9	−2.5	2.5	FAT10	S111
−3.2	−3.5	−1.4	−2.9	FAM83H	S914
−2.6	−3.0	−1.2	−3.2	AKAP12	S627
−2.7	−3.1	−1.9	−1.2	FNBP1L	S488, S501
−2.7	−3.1	−1.9	−1.2	FNBP1L	S489, S501
−2.7	−2.5	1.4	1.4	LOXL2	S371
−3.2	−2.9	1.1	1.1	NuMA-1	S1225
−2.6	−2.6	−1.5	−1.7	SPECC1L	S385
−3.9	−4.5	−1.3	−1.0	H2BFS	Y38
−3.9	−4.5	−1.3	−1.0	H2BFS	S39
−2.6	−2.5	1.1	1.4	H2B	S37
−3.6	−4.2	−1.2	−1.1	H2B	S39
−5.2	−3.9	−1.3	1.0	polybromo 1	S681
−4.4	−3.4	1.1	1.0	RBMS1	S38
−4.4	−3.4	1.1	1.0	RBMS1	S40
−5.3	−3.3	−1.4	−1.1	cofilin 1	T25
−2.6	−3.3	1.1	1.2	DDX50	S239
−4.6	−3.0	1.0	1.1	MDH1	S241
−3.7	−6.4	−1.1	−1.5	MDH1	S242
−4.7	−4.9	1.0	−1.0	NKEF-B	S112
−4.2	−4.0	−1.6	−1.7	EPS8L2	S240
−2.9	−2.6	−1.2	−1.9	RALGPS1	T331
−7.1	−4.8	1.4	1.6	MYO9A	T41
−2.5	−3.0	−1.5	−1.1	cofilin 2	S24
−2.5	−3.0	−1.5	−1.1	cofilin 2	T25
−2.6	−2.8	1.3	−2.1	NFAT1	S363
−3.2	−2.9	1.0	1.3	TFIIS	S57

Table S1. Cont.

K457 AKAP12 shRNA#5/K457 Scram shRNA	K457 AKAP12 shRNA#2/K457 Scram shRNA	K457 AKAP12 shRNA#5/K457 Scram shRNA	K457 AKAP12 shRNA#2/K457 Scram shRNA	Protein	Phosphorylation
−2.6	−6.7	−1.4	−1.1	TFIIS	T58
−2.8	−3.1	1.4	1.9	ZNF800	S317
−3.5	−4.0	1.1	1.7	ZNF800	T319
−2.7	−4.6	1.1	1.6	RPL34	Y13
−4.2	−2.7	2.3	1.7	1520402A15Rik	S118
−4.5	−3.0	1.4	−1.2	KIAA1468	S180
−1.1	2.7	−27.5	−21.7	MAP4	S823
1.2	2.3	−5.8	−8.5	MAP4	S827
1.4	−1.0	−6.9	−7.2	CDCA5	T159
−1.3	−1.0	−3.1	−3.0	KI-67	T1747
−1.4	−1.5	−2.9	−2.6	KI-67	S2223
1.4	−1.0	−6.9	−7.2	SPECC1L	S832
−2.0	2.1	−15.0	−5.3	HSP90B	S615
−1.0	−1.2	−5.0	−3.2	REPIN1	T567
−1.4	−2.9	−2.7	−2.5	TIP20	T89
1.5	1.2	−3.5	−2.9	lamin A/C	S17
1.5	1.2	−3.5	−2.9	lamin A/C	S22
−1.4	−2.3	−3.4	−3.0	lamin A/C	S390, S392
−1.4	−2.3	−3.4	−3.0	lamin A/C	S390, T394
−1.4	−2.3	−3.4	−3.0	lamin A/C	S390, S395
1.7	1.6	−24.6	−3.7	vimentin	S25, S27
1.4	1.0	−8.8	−4.0	vimentin	S51
−1.8	−1.3	−2.9	−3.2	Rab34	S241
1.1	−3.1	−11.0	−6.6	ARHGAP15	T21
2.0	−1.1	−2.8	−4.5	Cdc25B	S323
−2.0	−2.6	−3.2	−4.3	B-Raf	T401
1.8	1.9	−6.8	−7.9	CDK17	S122
1.8	1.9	−6.8	−7.9	CDK17	T124
−1.1	−1.6	−2.7	−3.2	PLK1	T210
−1.1	−1.6	−2.7	−3.2	PLK1	T214
1.5	−1.2	−4.8	−3.9	sialophorin	T343
1.4	1.1	−2.8	−7.2	GAS7	S152
−1.7	−1.6	−2.9	−3.1	LBH	S63
1.0	−1.3	−2.6	−2.9	ZNF24	T330
1.1	−1.2	−2.6	−2.7	NDRG1	S364, T375
1.7	1.2	−4.1	−2.6	NDRG1	T366, S367
1.1	−1.2	−2.6	−2.7	NDRG1	T366, T375
1.1	−1.2	−2.6	−2.7	NDRG1	T366, S378
1.1	−1.2	−2.6	−2.7	NDRG1	T366, S384

Table of normalized fold changes of the ratio of shRNA5/shScram and shRNA2/shScram phosphorylation under normoxia (21% O_2) and hypoxia (0.5% O_2). Green represents increased phosphorylation and red represents decreased phosphorylation (shAKAP12/shScram). Only substrates that acted similarly under both shRNAs are included in the table.

Dataset S1. Relevant kinases responsible for kinome-wide phosphorylation changes

Dataset S1

GPS 2.1.2 program was used to predict kinase-specific phosphorylation of each identified AKAP12-dependent phosphoprotein by conserved target motif and local amino acid physical characteristics (listed by high score and distance from the projected threshold). A high cutoff was selected with estimated false-positive rates of 2% for serine/threonine kinases and 4% for tyrosine kinases. A score >2 is statistically significant.